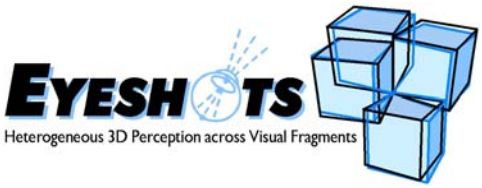

Project no.: FP7-ICT-217077
Project full title: Heterogeneous 3-D Perception across Visual Fragments
Project Acronym: EYESHOTS
Deliverable no: D3.3b
Title of the deliverable: Final fully tested version of the Working Memory Model

Date of Delivery:	25 March 2011	
Organization name of lead contractor for this deliverable:	WWU	
Author(s):	F.Beuth, H.Schroll, J.Vitay, F.Hamker	
Participant(s):	WWU	
Workpackage contributing to the deliverable:	WP3	
Nature:	Report	
Version:	1.2	
Total number of pages:	29	
Responsible person:	Fred H. Hamker	
Revised by:	Giorgio Cannata	
Start date of project:	1 March 2008	**Duration:** 36 months

Project Co-funded by the European Commission within the Seventh Framework Programme		
Dissemination Level		
PU	Public	**X**
PP	Restricted to other program participants (including the Commission Services)	
RE	Restricted to a group specified by the consortium (including the Commission Services)	
CO	Confidential, only for members of the consortium (including the Commission Services)	

Abstract:
This deliverable demonstrates the interaction of an enhanced version of our working memory model (D3.3a) and the object recognition system (D3.2). The working memory is achieved by recurrent loops between the subcortical areas of the basal ganglia and the prefrontal cortex. A similar loop through the motor cortex models a response selection behavior. The previous model in deliverable D3.3a did not learn the updating of working memory. The new model covers the biological structure of the mammal brain for the purpose of actively maintaining and updating the content of the working memory. One of the goals in Eyeshots is to develop a "perceptual agent for interacting, control/planning in the peripersonal space" using stereoscopic object recognition. Such complex tasks will at some point benefit from the ability to hold previously visible information in memory and to select between behavioral alternatives. Since not particularly task has been specified we used for this report a typical working memory task (the 1-2-AX task): The model is required a number of objects and select a category depending on the sequence of presented objects. As previously, the objects are modeled as 3D objects in virtual reality to allow stereoscopic object recognition. The recognition transforms the stereoscopic images into a cortical representation of the object. The basal ganglia model learns to memorize an object or to suppress it from working memory depending on the task requirements. It also learns to select the correct category based on previous received reward (stimulus-reward-associations).

Contents

1 Executive summary

This document contains the report for deliverable D3.3b "Final, fully tested version of the Working Memory Model". Technical report.

The European project "Eyeshots" focuses on the research of a visuo-motor system which is based on the concept of "active and fragmented vision". It is inspired by the primate brain which actively generates a cognitive interpretation of a perceived scene. It does not encode the scene as pure 2D images or reconstruct real 3D data. Instead, it creates an efficient code in which a scene consists of distributed and loose features, called visual fragments. A visual fragment can represent simple features (like edges or corners) or more complex parts of an object. A set of fragments is associated with each object and thus forms this object.

One of the goals of the project Eyeshots, sharing a peripersonal workspace, requires to hold previously visible information in memory to allow the agent to be able to choose between behavioral alternatives. Both requirements are addressed by the working memory model. We present the results achieved by a combined model of our object recognition system (D3.2) and of our working memory model (D3.3a). To ensure that the task is general enough and also replicable, we decided to use a well known task from literature of working memory. In this 1-2-AX task, decisions must be taken dependent on previously

presented symbols and the agent must be able to deal with distractors (distractors are irrelevant objects for the current task which should not be remembered). Only special combinations of the symbols (e.g. a '1', followed by 2 and by X) result in one certain decision, all other combinations result in another behavioral alternative. The number of possible combinations is very high and the agent does not know in advance if a symbol is important or a irrelevant. This is also typical for real world tasks which makes such tasks very difficult.

2 Combined model

2.1 Introduction

In this document, we demonstrate the interaction of a working memory model (D3.3a, [2, 4]) and the object recognition system (D3.2, [3, 5]). We have explored in deliverable 3.2 how the brain can bind different visual fragments together to form an object (binding process). A visual fragment can encode simple features like edges, but also more complex shapes like part of a view from an object. A set of fragments is associated with each object and thus forms this object. Our approach is that the concept of attention [6] is used to bind these spatially distributed fragments together. The attention process uses feedforward connections to detect the fragments and recognize an object. We do not use here feature-based attention (like in [3]) in form of feedback connections from the object representing cells to the feature cells.

Almost every task requires to hold previously visible information or to recall context information from memory, especially when the sharing of workspace is required. Such properties of cognitive vision systems are often referred to establishing a global workspace for specific tasks such as planning and action control. Working memory (WM) is a key prerequisite for planning and executing action responses. In a prominent notion [7, 8], WM consists of the capability to maintain information over limited periods of time and the capacity to manipulate that information. By maintaining information in WM, an organism can detach its responses from its immediate sensory environment and exert deliberate control over its actions. Healthy human adults demonstrate an enormous flexibility in WM control which must be acquired meticulously over many years of childhood and adolescence. In the early years of childhood, even WM tasks as simple as a Delayed-Match-to-Sample task pose a serious challenge [9, 10].

Several brain structures have been shown to contribute to WM, among them lPFC[1] [11, 12], posterior parietal cortex [13, 14], hippocampus [15], cerebellum [16] and BG[2]

[1] lPFC: lateral prefrontal cortex
[2] BG: basal ganglia

[17, 18]. We focus here on the role of a looped architecture of cortex, BG and thalamus in controlling WM and motor selection: Closed cortico-BG-thalamic loops, connecting a particular area of cortex to itself, can be anatomically distinguished from open loops, linking in an ascending manner areas involved in motivation, action planning and motor execution [19, 20]. This architecture of parallel and hierarchically interconnected loops provides a potential anatomic substrate for how cognitive and motor states can be maintained for extended periods of time (closed loops), and for how cognitive processes can bias response selection (open loops; cf. [19]).

The prominent role of BG within cortico-BG-thalamic circuitry has been conceptualized in several theoretical accounts: BG are assumed to take part in visual and motor category learning [21], in transforming goal-directed actions into habitual responses [22, 23] and in establishing associations between stimuli and responses [24]. Most eminently for learning of behavioural alternatives, BG has an important role in reinforcement learning[3]: BG receive dopaminergic afferents from SNc[4] providing the BG with an error signal of reward prediction [25, 26, 27]. This reward prediction error is encoded by Dopamine levels which have been shown to modulate long-term synaptic plasticity within BG, especially in its major input structure, the striatum [28, 29, 30]. Functional, Dopamine can be seen as an reward prediction error, encoding the difference between the expected and the currently received reward. Dopamine bursts (above a tonic baseline level) occur from unexpected rewards while dopamine depletions (under this baseline) follow omissions of expected rewards.

In summary, the report will focus on the integration of the object recognition system with the developed and recently improved working memory model. The object recognition system will only be mentioned briefly (a comprehensive description can be found in [3, 5]) and we will focus in this report on the biological enhancements of the working memory model. We will present a biologically meaningful computational model of how the BG-loops contribute to the organization of working memory and the development of response behavior. The model learns to flexibly control working memory within prefrontal loops and to select appropriate responses based on working memory content and visual stimulation within a motor loop. Importantly, we show that both systems, working memory control and response selection can, develop on top of the same cortico-basal ganglio-thalamic architecture by Hebbian and Dopamine based three-factor learning. As a exemplary working memory task for a shared workspace scenario, we use the relatively complex 1-2-AX task and we describe that we must teach the task in three steps (Shaping), otherwise it can not be learned by the model nor by humans or animals [33]. In general, humans are able to learn very complex task also only step by step and we show that the model can deal with such a complex tasks in the same way. Finally, we will

[3]RL: A mammal is trying a behaviour and it learns from its received reward.

[4]SNc: substantia nigra pars compacta, a nucleus of the midbrain

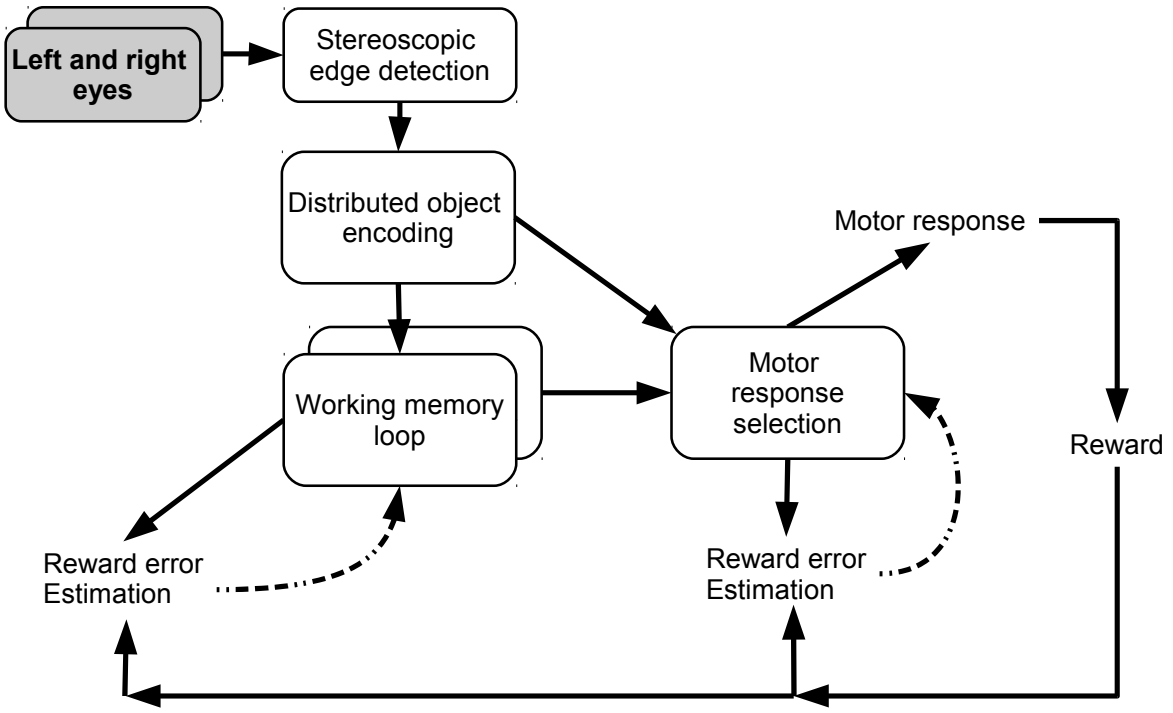

Figure 1: Functional overview of the combined object recognition (stereoscopic edge detection and distributed object encoding) and working memory model (working memory loop and motor response selection). Dashed lines indicate Dopamine influence, therefore these weights are adapted according to the difference between received and expected reward (reward estimation error).

demonstrate the enhanced model ability to learn the 1-2-AX task after combination with object recognition. Parts of this deliverable are taken from the manuscript "Working memory and response selection: A computational account of interactions among cortico-basal ganglio-thalamic loops" by Schroll *et al.*, 2011 ([1]). The manuscript contains a comprehensive description of the model (including all equations) and the performance for two working memory tasks (delay response and 1-2AX).

2.2 Functional overview about the combined model

The goal of the model is to maintain working memory and to select the correct response for the current task. It learns from visual experience and from previous rewards by associating these rewards to specify visual stimuli. The central idea of maintain the working memory is that an agent has to remember objects that are useful or necessary for the task at hand. An object can be defined as very useful, if the agent can expect a high

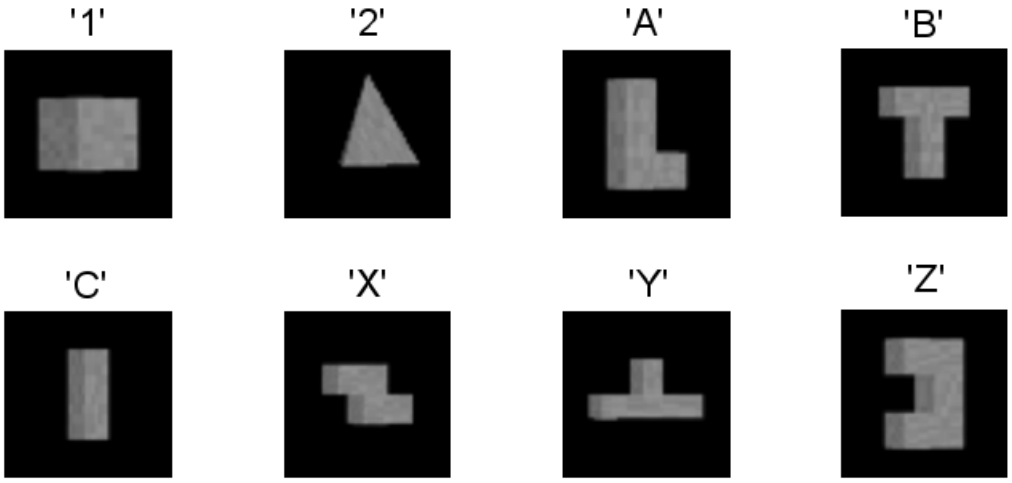

Figure 2: The stimuli consist of 8 different 3D objects representing the 8 symbols used in the 1-2-AX task [33]. The letters at the top denotes the symbol names of the 1-2-AX task.

reward when it remembers this object and choose a decision based on this memorization. By this idea, the agent learns when it should store, hold or delete a specific stimuli from WM.

Figure 1 gives an overview of the model. We have built in a virtual reality(VR) 8 different objects, each represents a symbol for the 1-2-AX task (Figure 2). The VR raytracer creates stereoscopic views of these 3D objects. First, the views are processed by an stereoscopic edge detection model. From this representation, the system recognizes an object and represents it in a distributed way, hence every symbol is encoded by several cells. After recognizing the object, we pass the activations to the WM and motor response selection system.

The working memory is organized in several thalamic-cortex-BG loops which can each maintain a certain symbol. The basal ganglia system estimates the expected reward for each symbol. If we get more reward than expected, the model reinforces the memorization of such a loop, therefore the object was helpful to solve the current task. If the object will occur again, the working memory will memorize it and the model will be able to solve the task again. On the opposite, if the model receives less reward than expected, the model has remembered the wrong object resulting in an inhibition of specific weights and the model will less likely store the symbol in working memory in the future. The difference between expected reward and received reward is called reward prediction error and the function of this term can be compared to Dopamine release in the brain [25, 26, 27]. The model will learn which symbol is useful for a task, but it will learn as well which symbol should be suppressed from working memory content.

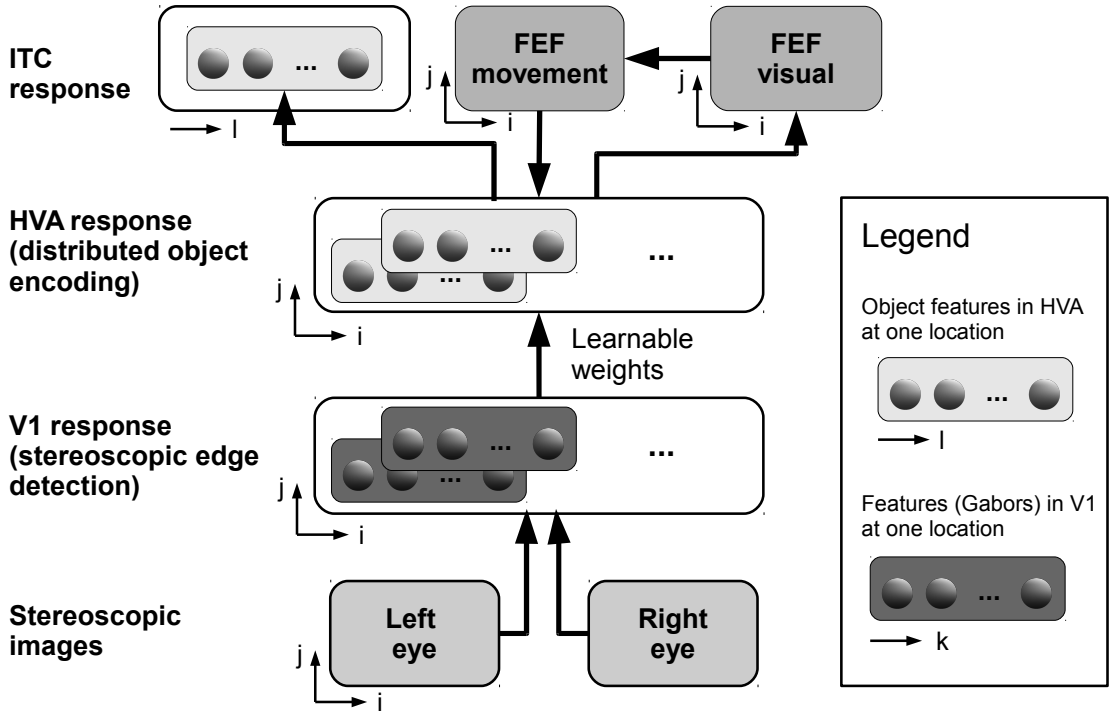

Figure 3: Neuronal network of the stereoscopic object recognition model. The i and j indices correspond to the spatial x and y axis of the images. The index k refers to different Gabor responses and l to different learned features in HVA. Adapted from [3].

From the current presented stimuli and the past sensations (WM), the model learns to associate a motor response. This learning is again based on the expected and received reward. At the beginning, the working memory can not be maintained appropriate and the motor decisions can only be chosen dependent on the currently presented symbol. After the agent gets constantly rewarded, the model learns to maintain WM accurately. Because of these requirements, the motor-reward association are learned faster and perform earlier correctly than the working memory loops.

After this functional overview about the model, we briefly introduce the object recognition system and then explain the biological architecture of the basal ganglia system to achieve a biological meaningful WM model.

2.3 Object recognition system

The object recognition system [3, 5] uses learned object representations based on local edge detectors. The objects are detected depending on their shape or texture and thus we do not use color information. The following section is a summary of Beuth *et al.* (2010). In our neuronal model (Fig. 3), we simulate an early area (V1) detecting stereoscopic edges and a high level area (HVA) recognizing objects. The cells of HVA could be functional mapped onto area V2/V4/ITC. An object is represented by a distributed code of HVA cells, where a single HVA cell can be interpreted as representing a single view of an object. As input stimuli we use the left and right eye view of 8 different 3D objects (Fig. 2), produced by a raytracer engine [34]. The first layer serves as a preprocessing for the HVA, it detects stereoscopic edges and disparities via an energy model [35, 36, 37] and it is comparable to area V1. This particular energy model [38] uses 56 Gabors with 8 orientations (with a $\frac{\pi}{8}$ step size) and 7 different phase disparity shifts (with $\frac{\pi}{4}$ step size). This area builds a representation of the scene encoding edge information, independent of the right or left view and therefore enables stereo object recognition.

Overlapping receptive fields serve as input for the cells of the HVA. We achieve the object selectivity by learning the feedforward weights (V1$\rightarrow$ HVA) with a biological motivated learning algorithm [39] and a trace rule using temporal continuity for the development of view-invariant representations of objects (like in [40, 41, 42]). For the idea of trace learning, we use the temporal correlations which are included in the visual input. If we consider a short time spawn, mammals will look with a higher probability at the same object rather than at different objects. Therefore, the visual input is more likely to originate from different views of the same object, rather than from a different object. To combine stimuli that are presented in succession to one another, activation of a pre-synaptic cell is combined with the post-synaptic activation of the previous stimulus using the Hebbian principle. We simulated an appropriate temporal presentation protocol where the agent mostly kept the fixation at one object and only rarely switched to another object.

The Frontal Eye Field (FEF) consists of two areas, the saliency map (called FEF visual) and the map encoding the target of the next eye movement (called FEF movement). One of the binding processes operates over all locations in HVA and reinforces the features of the searched object (which depends on the current task). The other is achieved by the loop over FEFvisual and FEFmovement. This mechanism reinforces adjacent locations. Both processes use a soft winner takes all competition to decrease the activity of irrelevant features and locations in HVA. After convergence of the system, FEFmovement encodes the target of the next planned saccade. From this information about the object position, we can use the appropriate HVA response as a distributed neuronal response

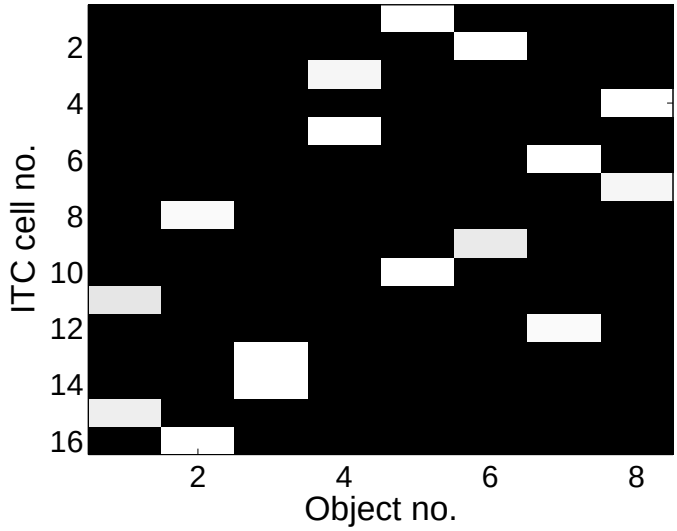

Figure 4: The input of the working memory part of the combined model. The neuronal reponse of ITC is shown for every symbol (at the x-axis) and every cell of ITC (y-axis). Comparing to the original model, the combined model uses a biological more realistic distributed representation of the symbols.

to represent the object. This neuronal response (Figure 4) is comparable of the neurons in ITC and it will be directly passed to the WM and response selection model.

2.4 Distributed representation of symbols in the combined model

The combination of the object recognition system with the WM model made a change of the symbol representation in ITC necessary. In the combined model, each object is represented by several cells in a distributed manner. The encoding is the same as used for the object representation in the HVA (Figure 3) and more precisely, it is determined by the feedforward weights (V1→ HVA). These weights are learned from the visual information by the trace learning rule [3] in a self-organized manner and and hence the encoding of the cells is indirectly determined by the visual input.

Due to the distributed coding we increased the overall number of cells in ITC, here from 8 to 16 (arbitrary chosen value). The working memory model uses the object encoding of ITC as input. Most connections are adapted by Hebbian learning or by Dopamine learning. Both learning rules can deal with an increased number of cells due their self organizing principle. To conclude, the model works well with different input sizes if the mean activity in the areas ITC, PFC, STN, GPe are nearly the same. It is of course

necessary that the firing rates of active cells in ITC can clearly distinguish from inactive cells.

3 A model for working memory and response selection

This section briefly describes the enhanced working memory model (WM model) focusing on the biological architecture.

3.1 Biological architecture of the model

BG can be divided into three main functional domains based on cortico-striatal afferents [44]. 1) The limbic/ ventral domain is involved in classical conditioning and evaluation of motivational valences [45]. The corresponding part of the striatum is called nucleus accumbens and receives afferents from orbitofrontal cortex, amygdala and hippocampus. 2) The executive domain (associated to the caudate nucleus as another part of striatum) is mainly connected to lPFC. It is involved in goal-directed learning, action-outcome associations and WM [46]. 3) The sensorimotor domain is mainly associated to premotor and sensorimotor cortices and is involved in action selection, stimulus-response associations and habitual control [47]; the corresponding striatal part is called putamen. These different domains interact through ascending cortico-cortical projections, thalamo-cortico-thalamic projections and through a spiraling pattern of connections between striatum and the dopaminergic areas of SNc and ventral tegmental area [19]. Further, cortico-striatal fibers that originate from different cortical areas overlap in the striatum [49, 48, 50]. These anatomical arrangements create a hierarchy of information flowing from the limbic domain via the executive/prefrontal domain to the sensorimotor domain. [19]. Figure 5 shows the general layout of our model which contains two prefrontal loops and one motor loop. The model consists of parallel and hierarchically interconnected loops that have the same general architecture and obey the same learning rules. The loops' internal connectivity is consistent with cortico-BG-thalamic circuitry [51, 32, 19]. Prefrontal cortico-BG-thalamic loops (as shown on the left of Figure 5) control WM by flexibly switching between maintenance and updating of information. Then, they bias a motor loop (shown on the right of Figure 5) to decide between a set of possible responses. As previously motivated by others (e.g. [33, 43, 52]), our model contains multiple independent prefrontal loops. While there is no theoretical limit to the number of loops that can be incorporated, we kept it as small as possible to minimize computational costs: two loops are sufficient to learn the task analyzed in this report.

The general functional framework of our model is straightforward. During stimulus

presentation, visual input is externally fed into ITC[5]. Stimulus-related activity can then spread through the model and bias processing within prefrontal and motor loops. Motor responses are read out of MI[6] activity and rewarded if correct. When a reward is given, reward information is fed into SNc where an error signal of reward prediction is computed. From this error signal, BG learn to self-organize in such a way that the model's responses maximize rewards.

All cortico-BG-thalamic loops obey the same functional architecture. Notice, however, that the motor loop is simplified in some respects when compared to prefrontal loops: it is not equipped with a hyperdirect pathway and has hard-coded instead of learnable pallido-pallidal, cortico-thalamic and thalamo-cortical connections. For the tasks analyzed in this report, these simplifications do not result in significant reduction of model performance while on the other hand saving computational resources. The loops' functional architecture works as follows. Activation in the cortex excites striatal and subthalamic neurons. Striatum then inhibits tonically active neurons of GPi[7] via striato-pallidal connections that are usually referred to as the direct BG pathway. Decreasing of GPi firing in turn disinhibits thalamic neurons that excitatorily connect back to cortex. In global terms, the direct pathway serves both to establish WM maintenance by mapping cortical representations onto themselves, and to link WM content to appropriate responses by mapping prefrontal-loop representations onto specific motor-loop representations. In contrast, activation of STN[8] causes a strong and global excitation of GPi via subthalamo-pallidal fibers that are usually referred to as the hyperdirect pathway. As activity is spreading from STN to GPe[9], inhibitory GPe-GPi connections cancel the excitatory effects of STN on GPi. In prefrontal loops, the hyperdirect pathway thus gives a brief and global reset pulse to GPi, allowing the respective loop to update. As stated above, we did not model the hyperdirect pathway of the motor loop which we assume to hold back motor responses until appropriate. The interplay of the various layers is in detail be analyzed in [1], section 3.2.2.

Each of the modeled layers consists of dynamic, firing rate-coded neurons (exact numbers are reported in [1], Table C.2). For each neuron, a membrane potential is determined by a differential equation, discretized according to the Euler method with a timestep of 1 ms; a cell-specific transfer function turns membrane potentials into firing rates. The differential equations are evaluated asynchronously to allow for stochastic interactions between functional units. As a general template, membrane potentials $\left(m_i^{\text{post}}(t)\right)$ are

[5]ITC: inferior temporal cortex
[6]MI: primary motor cortex
[7]GPi: globus pallidus, internal segment
[8]STN: subthalamic nucleus
[9]GPe: Globus pallidus, external segment

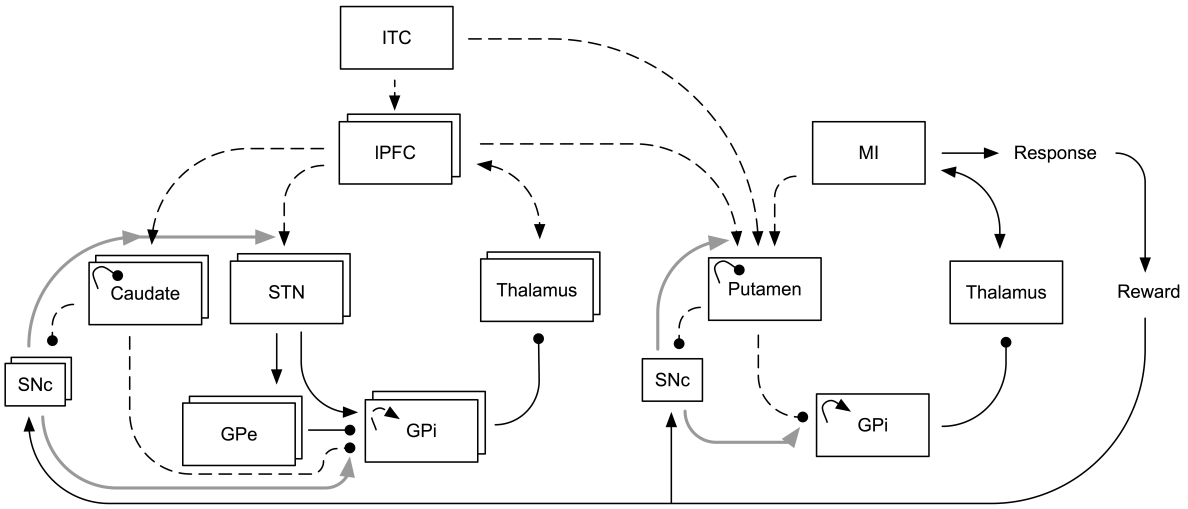

Figure 5: Architecture of the working memory model: prefrontal cortico-BG-thalamic loops flexibly control WM and guide a motor loop to choose between a set of possible responses. While the general layout of prefrontal and motor loops is the same, the motor loop is simplified as explained in the main text. Boxes represent the different layers of the model, arrows the connections between them. Solid arrows denote hard-coded connections between or within layers, dashed arrows learnable ones. Pointed arrows symbolize excitatory connections, rounded arrows inhibitory ones. The grey arrows deriving from SNc represent a modulatory influence on learning within BG afferents. Explanations are given in the main text. GPe: globus pallidus external segment; GPi: globus pallidus internal segment; lPFC: lateral prefrontal cortex; MI: primary motor cortex; ITC: inferior temporal cortex; SNc: substantia nigra pars compacta; STN: subthalamic nucleus.

computed by the following differential equation:

$$\tau \cdot \frac{dm_i^{\text{post}}(t)}{dt} + m_i^{\text{post}}(t) \;=\; \sum_{j \in \text{pre}} w_{i,j}^{\text{pre}}(t) \cdot u_j^{\text{pre}}(t) + M + \epsilon_i(t) \tag{1}$$

where: τ is the time constant of post-synaptic cell i, $u_j^{\text{pre}}(t)$ the firing rate of presynaptic cell j, $w_{i,j}^{\text{pre}}(t)$ the weight between these cells, M a baseline membrane potential and $\epsilon_i(t)$ a random noise term. Each of the cell's inputs is determined by multiplying the respective presynaptic firing rate by the weight from the pre- to the post-synaptic cell. Individual inputs are then summed up and the baseline membrane potential and random noise term are added.

Firing rates $\left(u_i^{\text{post}}(t)\right)$ are computed from membrane potentials by a layer-specific transfer function, usually giving the positive part of the membrane potential:

$$u_i^{\text{post}}(t) \;=\; \left(m_i^{\text{post}}(t)\right)^+ \tag{2}$$

with $()^+$ denoting that negative values are set to zero.

Loops are not predetermined to represent particular stimuli: each prefrontal loop receives the same visual input and only by accumulating knowledge about its environment it will learn to encode certain stimuli and ignore others. Figure 5 depicts all learnable connections of the model by dashed arrows. As explained in detail in the next paragraphs, thalamo-cortical and cortico-thalamic learning is Hebbian-like whereas learning in BG relies on three-factor rules, involving presynaptic, post-synaptic calcium level and a reward-related dopaminergic term [53]. Dopamine levels are controlled by SNc firing rates and encode an error signal of reward prediction.

Dopaminergic learning poses an obvious challenge on modeling: the stimuli are typically presented (and responses performed) before reward delivery (compare section 4.1), there will be a delay between concurrent activity of pre- and post-synaptic cells and the dopamine levels resulting from that activity. The brain's probable solution to this problem is the usage of synapse-specific calcium eligibility traces: concurrent pre- and post-synaptic activity leads to a sudden rise in input-specific post-synaptic calcium concentrations $\left(\text{Ca}_{i,j}^{\text{post}}(t)\right)$ that decrease only slowly when concurrent activity ends.

$$\eta^{\text{Ca}} \cdot \frac{d\text{Ca}_{i,j}^{\text{post}}(t)}{dt} \;=\; \left(u_i^{\text{post}}(t) - \overline{\text{post}}(t)\right)^+ \cdot \left(u_j^{\text{pre}}(t) - \overline{\text{pre}}(t)\right) \tag{3}$$

$$\eta^{\text{Ca}} \;=\; \begin{cases} \eta^{\text{inc}} & \text{if } d\text{Ca}_{i,j}^{\text{post}}(t) > 0 \\ \eta^{\text{dec}} & \text{else.} \end{cases} \tag{4}$$

η^{Ca} is the time constant of the calcium trace, $\overline{\text{pre}}(t)$ the mean firing rate of afferent layer *pre* at time t, $\overline{\text{post}}(t)$ the mean firing rate of post-synaptic layer *post* at time t, η^{inc} a

parameter controlling the speed of calcium level increase and η^{dec} a parameter controlling the speed of calcium level decline. When, at the same point of time, both presynaptic cell j and post-synaptic cell i fire more than the mean activities of their respective layers, $d\text{Ca}_{i,j}^{\text{post}}(t)$ gives a positive value. As η^{Ca} is set to the relatively small value of η^{inc} in that case, the corresponding calcium level increases rapidly. In contrast, when concurrent activity ceases, $d\text{Ca}_{i,j}^{\text{post}}(t)$ becomes negative and the calcium level decreases. As η^{Ca} is set to a relatively large value (η^{dec}) in that case, it does not directly drop to zero but declines rather smoothly. Calcium eligibility traces are inspired by findings that calcium levels stay heightened for some interval longer than actual pre- and post-synaptic activity [54] and that post-synaptic calcium is required for striatal dopamine-mediated learning [55, 56]. Specificity of synaptic plasticity is an established finding [57].

To determine the change in BG-afferent weights $\left(w_{i,j}^{\text{pre}}(t)\right)$, a three-factor learning rule is used, comprising the calcium trace described above (which contains the two factors pre- and post-synaptic calcium levels) and a dopaminergic term ($\text{DA}(t)$) linked to reward delivery:

$$\begin{aligned} \eta \cdot \frac{dw_{i,j}^{\text{pre}}(t)}{dt} &= f\left(\text{DA}(t) - \text{DA}_{\text{base}}\right) \cdot \text{Ca}_{i,j}^{\text{post}}(t) \\ &\quad -\alpha_i(t) \cdot \left(u_i^{\text{post}}(t) - \overline{\text{post}}(t)\right)^2 \cdot w_{i,j}^{\text{pre}}(t) \end{aligned} \tag{5}$$

$$\tau \cdot \frac{d\alpha_i(t)}{dt} + \alpha_i(t) = K_\alpha \cdot \left(u_i^{\text{post}}(t) - u^{\text{MAX}}\right)^+ \tag{6}$$

$$f(x) = \begin{cases} x & \text{if } x > 0 \\ \phi \cdot x & \text{else.} \end{cases} \tag{7}$$

$\text{DA}(t)$ is the dopamine level of the respective loop at time t, DA_{base} the baseline dopamine level of 0.5, $\alpha_i(t)$ an adaptive regularization factor, u^{MAX} the maximal desired firing rate of cell i, ϕ a constant regulating the strength of LTD[10] relative to the strength of LTP[11] and K_α a constant that determines the speed of increases of $\alpha_i(t)$. In case of a dopamine burst (i.e. when dopamine levels rise above the baseline level of 0.5), all weights are increased in proportion to the strengths of their calcium traces; dopamine depletions (i.e. dopamine levels below baseline) decrease recently active synapses accordingly. The subtractive term of the equation ensures that weights don't increase infinitely: when connections are strong enough to push firing of a post-synaptic cell above a particular threshold defined by u^{MAX}, α_i increases and all weights to that post-synaptic cell are diminished. Increases of α_i can be slow or fast depending on the value of K_α.

By applying a single set of learning principles to all loops, we show their flexibility to implement two highly different functions: to establish flexible control of WM, and to

[10]LTD: long-term depression
[11]LTP: long-term potentiation

link distinct cortical representations in a stimulus-response manner, thereby linking WM to motor control. While the general learning rules for prefrontal and motor loops are the same, the parameter values regulating LTD in case of dopamine depletion differ. In particular, LTD in prefrontal loops is assumed to be slower than in the motor loop, biologically inspired by a gradient of rostro-caudal dopamine D2 receptor density that increases from limbic via associative to sensorimotor striatum [58, 59]. Functionally, this parametric difference ensures that after a sudden change in reward contingencies (resulting in dopamine depletions), re-learning in the motor loop is faster than re-learning in prefrontal loops: attempts to map priorly relevant stimuli onto different responses will thus be undertaken faster than gating previously irrelevant stimuli into WM.

The following paragraphs will focus on the different functional parts of the model and explain the supposed architecture more thoroughly.

3.1.1 Cortex

The WM model contains lPFC and MI. lPFC is assumed to take part in WM control, presumably being involved in both active maintenance and manipulation of information [60]; MI integrates cortical and subcortical inputs to send an emerging motor command directly to the motoneurons of the spinal cord [61]. We here simplify lPFC and MI to represent visual stimuli and motor commands by single neurons. However, Vitay and Hamker [62] provide a computational framework to understand how more realistic distributed cortical representations interact with subcortical brain structures. All cortical cells receive excitatory thalamic input. lPFC additionally receives cortico-cortical afferents from ITC that are involved in visual object recognition [63].

Cortico-cortical and thalamo-cortical connections are defined to be learnable. Learning of the corresponding weights is assumed to be Hebbian-like. Although there is empirical evidence of dopaminergic innervation of prefrontal cortex, the corresponding dopamine signals are not well suited to reinforce particular stimulus-response associations as they have been shown to last for several minutes [31, 64].

3.1.2 Thalamus

Thalamus is assumed to relay information to cortical areas [65] and to control cortical activation and deactivation [66]. Consistent with this, maintenance of a representation in WM and selection of a response requires thalamic disinhibition through GPi in the model. Thalamic cells receive inhibitory pallidal and excitatory cortical input (cf. Figure 5). As with prefrontal cortex, there is evidence for dopaminergic innervation of the thalamus [67, 68]. The nature of the dopamine signals provided, however, has not yet

been clearly elucidated. Conservatively, we thus assume cortico-thalamic learning to be Hebbian-like (i.e. not to be modulated by dopamine).

3.1.3 Striatum

There are two input structures of BG: striatum and STN. Both receive glutamatergic cortical afferents and both are organized topographically [69, 70]. Striatum can be subdivided into putamen, receiving mostly motor-cortical afferents, and caudate nucleus, innervated by lPFC [44]. Next to excitatory cortical afferents, striatal cells receive inhibitory input from a network of GABAergic interneurons [71]. In the model, these are hard-coded for means of simplicity and serve to downsize the number of striatal cells that become associated to each cortical representation. Activity of caudate nucleus has been shown to be negatively correlated with progress in reward-related learning [72]. Lesioning dorsolateral parts of the striatum leads to disabilities in stimulus-response learning [73]. Within the model, striatum learns to efficiently represent single or converging cortical afferents in clusters of simultaneously activated cells as shown in Vitay and Hamker [2]. Striatum gives rise to the direct BG pathway, connecting striatal cell clusters to single GPi cells. Thereby, it is vital both for WM maintenance and stimulus-response learning.

3.1.4 Subthalamic nucleus

STN is considered part of the hyperdirect BG pathway, linking cortex with GPi by two excitatory connections [74]. Also, STN excitatorily innervates GPe [75]. Recently, STN has become a key target structure for DBS[12] in Parkinsonian patients in order to alleviate dyskinesia [76] and to improve mental flexibility [77, 78]. STN DBS has been reported to cause WM deficits in spatial delayed response tasks [79] and n-back tasks [80], thereby further underlining its contribution to cognitive processing. Electrical stimulation of STN in monkeys yields a short-latency, short-duration excitation of GPi, followed by a strong inhibition, the latter being mediated by GPe [81]. Based on these findings, we assume STN within prefrontal loops to give a global (learned) excitatory reset signal to GPi that is cancelled by STN-GPe-GPi fibers shortly after.

3.1.5 Globus pallidus external segment

The role of GPe in BG functioning is still rather elusive. Historically, GPe has been considered a relay station on a striato-GPe-subthalamo-GPi pathway, often referred to as the indirect BG pathway [82, 83]. More recently, such a simple notion has been challenged and GPe has been hypothesized to have a more prominent processing function in

[12]DBS: deep brain stimulation

BG [84]. Anatomically, GPe is well-situated to take a central position in BG processing as it is connected bidirectionally with both striatum and STN and projects unidirectionally to GPi and thalamus [51]. Our model contains a reduced set of pallidal connections, accounting for afferents from STN and efferents to GPi only. Thereby, GPe is modeled only in its potential contribution to the hyperdirect (and not the indirect) pathway.

3.1.6 Globus pallidus internal segment

The internal segment of globus pallidus is a major BG output structure receiving and integrating subthalamic, external pallidal and striatal input [32]. GPi has a high baseline firing rate by which it tonically inhibits thalamic neurons [85]. Striatal and GPe inputs inhibit GPi cells below this baseline, thus disinhibiting thalamic neurons and opening a gate for mutually excitatory cortico-thalamic loops [32]. Subthalamic input in contrast excites GPi, thus further inhibiting thalamic neurons and preventing cortico-thalamic loops from firing [74]. The interplay of afferents to GPi which is critical for the model's functioning, is studied in detail in [1]., section 3.2.2.

Lateral competition in GPi ensures that each striatal cell cluster connects to a single pallidal cell only. While this is of course a simplification, it reasonably reflects the much smaller number of pallidal cells relative to striatal ones [86]. The lateral weights evolve according to an Anti-Hebbian learning rule.

3.1.7 Substantia nigra pars compacta

Inspired by the findings of Schultz and co-workers [25, 27] and in line with other computational accounts of reinforcement learning [e.g. 33, 87], we assume SNc neurons to compute an error signal of reward prediction. This signal is then relayed to BG to modulate learning of afferent connections. A detailed account of the underlying rationale can be found in Vitay and Hamker [2]. Briefly, SNc neurons compute a difference signal between actual and expected rewards and add the resulting value to a medium baseline firing rate of 0.5. Thereby, unexpected rewards lead to activity above this baseline while omissions of expected rewards result in a decrease in SNc firing. Information about actual rewards is set as an external input while stimulus-specific reward expectations are encoded in learnable striato-nigral afferents.

Each prefrontal and motor loop is connected to a separate SNc neuron. This is based upon reports showing SNc to have a topographical organization and reciprocal connections with striatum [88, 19]. Inspired by evidence showing SNc neurons to broadly innervate striatal subregions [89], we assume a single dopamine neuron to innervate all BG cells of a corresponding loop.

3.1.8 Pedunculopontine nucleus

As outlined above, the model contains multiple prefrontal loops. Following an idea of Krueger and Dayan [43], recruitment of these loops is dependent upon error detection after prior successful task performance. The framework of our model allows us to develop a biologically plausible mechanism of error detection: highly unexpected errors (i.e. errors after prior successful task performance) lead to a huge dip in SNc firing. This SNc signal can be used to recruit additional SNc neurons, thereby enabling learning within additional prefrontal loops. We assume an additional dopamine neuron to start firing whenever the most recently recruited neuron fires below a fixed threshold of 0.05. In contrast to the model of Krueger and Dayan [43], learning rates within previously engaged loops are not artificially decreased.

A potential anatomic substrate for subserving such a recruitment is a part of the brainstem named PPN[13]. PPN has been associated to the phenomena of attention, arousal, reward-based learning and locomotion [90, 91]; activation of cholinergic afferents from PPN to SNc has been shown to recruit quiescent dopamine neurons [92]. As PPN is innervated by many BG structures [93], it presumably also receives information about reward prediction. It might thus subserve a basic form of task monitoring, reacting whenever unexpected omissions of reward occur. Of course, the mechanism we propose may likely be largely simplified: other brain areas than the PPN have been linked to error detection as well, in particular the anterior cingulate [94]. Further, PPN output is not restricted to SNc but also reaches other BG nuclei, most notably STN [91]. Thus, PPN will neither be the only brain structure involved in error detection nor will recruitment of dopamine neurons be the only way it assists in modulating learning in cortico-BG-thalamic loops.

4 Model performance

This section describes the 1-2-AX task and investigates the task performance (the number of leaning steps required) of the combined model.

4.1 Experiment setup and 1-2-AX task

We use the relatively complex 1-2-AX task as an exemplary working memory task. In this task, a successive list of objects is presented as depicted in Figure 6. Within each trial, one of a set of possible stimuli (*1*, *2*, *A*, *B*, *C*, *X*, *Y* and *Z*) is shown and the agent is required to press one of two buttons. Only and exactly one of these buttons

[13]PPN: pedunculopontine nucleus

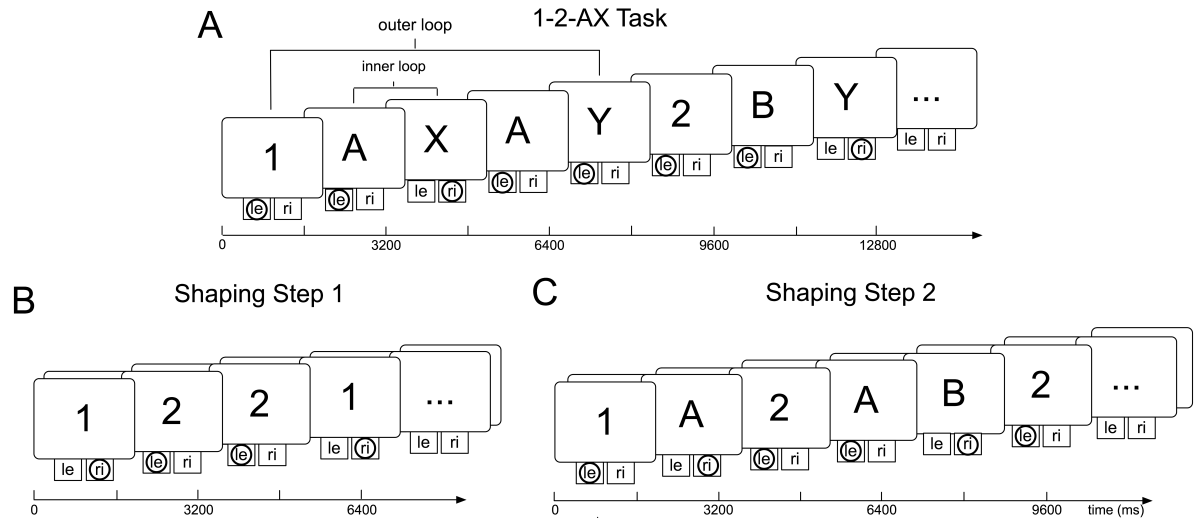

Figure 6: The 1-2-AX conditional WM task and the shaping procedure proposed to train the model. In each trial, a stimulus is presented and the model has to choose between a left- and a right-button press. Circles indicate correct responses. Please refer to the main text for detailed explanations. (A) Full 1-2-AX task. (B) Step 1 of the shaping procedure involving only the outer-loop stimuli *1* and *2*. (C) Step 2 of the shaping procedure involving outer-loop stimuli (*1* and *2*) plus inner-loop stimuli (A, B and C). le: left button; ri: right button.

will lead to reward when pressed. As mentioned earlier the numbers and letters stand for 3D objects. The task has a complex inner-outer loop structure that is not known to the model: numbers (*1* and *2*) represent context cues and constitute the outer loop. To correctly perform the task, the last outer-loop stimulus has to be kept in WM at any time. Whenever the last outer-loop stimulus has been a *1*, the letter X requires a right-button press if it has been directly preceded by an A; if the last outer-loop stimulus has been a *2*, a Y that directly follows a B requires a right-button response. In all other cases, a left-button press has to be performed. There are several versions of this task regarding the sequence of stimuli. We will here use the version employed by O'Reilly and Frank [33]: First, an outer-loop stimulus (i.e. *1* or *2*) is randomly chosen. Then, with equal probabilities, one to four inner loops are generated. With a probability of 0.5, an inner loop consists of a potential target sequence (i.e. A-X or B-Y); otherwise, any of the inner-loop stimuli (i.e. A, B or C) is followed by any of X, Y or Z, all probabilities being equal.

Teaching this task to the model requires a three step shaping procedure as depicted in Figure 6, otherwise the task can not be learned by the model nor by humans (given no further instructions and just being presented a sequence of objects) or animals [33]. In general, animals are able to learn very complex tasks only step by step and we show

that the model can solve such an problem in the same way. In a first step, only the outer-loop stimuli *1* and *2* are presented, probabilities being equal (Figure 6B). Each *1* requires a right-button press, each *2* a left-button press. When the model has reliably acquired this task (which is conservatively assumed to be the case after 100 correct responses in a row), the inner-loop stimuli A, B and C are added to the sequence. An outer-loop stimulus can be followed by one or two inner-loop stimuli, all probabilities again being equal. A right-button press is required for an A if the last number has been a *1* and for a B if the last number has been a *2*. In all other cases, a left-button press is required (Figure 6C). Finally, when the second step is securely coped with, the full task is presented (Figure 6A). After 150 correct responses in a row, the model is classified as having solved the task; if this criterion is not reached within 10000 trials, we admit that the model has failed. In the first two steps of shaping, stimulus presentation (lasting for 400ms) is separated from response requirement by a 400ms delay period. This is to ensure that the model learns to make use of WM, preventing it from solving the task by simply associating visual ITC representations to responses. By employing the latter strategy, the model would not develop the ability to maintain the stimuli in WM as is required to successfully master the subsequent steps of shaping. For the full task, responses are required while visual stimulation is still on as proposed by O'Reilly and Frank [33]. Each stimulus is presented for 800ms. 400ms after stimulus onset, the model is required to perform a response while the stimulus is still present.

4.2 Task performance

Figure 4.2 shows the performance of the combined model of 20 randomly initialized networks succesfully learning the 1-2-AX task. For each step of the shaping procedure, box plots show the number of trials needed until the last error occurs. Networks not learned the task to criterion were removed from the data for Figure 4.2. This occurs for approximate 25% of the networks.

Now, we investigate the learning of the different shaping steps closer. Two-sided Wilcoxon signed-rank tests provide difference statistics for the number of trials needed to cope with the different steps: The second step of shaping ($Mdn = 222, IQR = 84$) takes significantly longer than the first step ($Mdn = 101, IQR = 19,75$), $z = 3.62, p < .001$, as can be explained by the more complex set of rules to learn and the higher number of additional WM representations to develop. The third step ($Mdn = 313, IQR = 204$) requires significantly more trials than the first step of shaping, $z = 3.52, p < .001$ but does not differ significantly from the second step, $z = 1.58, p = .11$. In the third step, a highly complex set of rules has to be learned while no additional WM representations have to be developed.

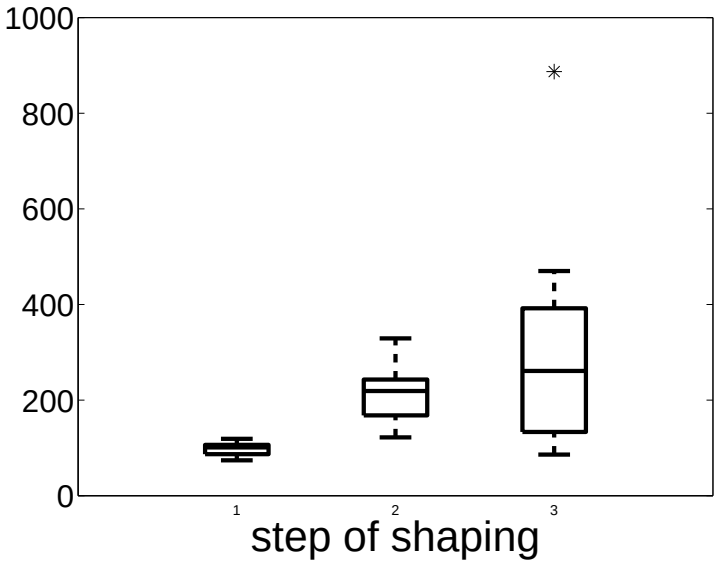

Figure 7: The the combined model's performance in learning of the WM task 1-2-AX. Combined model performance at the 1-2-AX task, separately for each step of shaping. Box plots show the number of trials needed until the last error occurs. The boxes' upper and lower borders represent upper and lower quartiles, respectively; the median value is shown as a line crossing each box. Whiskers extend to a maximal length of 1.5 times interquartile range, outliers are represented by asterisks.

5 Conclussion & future work

We have proposed a biologically computational model combining object recognition and reinforcement learning which lead to the organization of WM and overt response behavior. Our model demonstrates that both flexible control of WM and adaptive stimulus-response mappings can develop within parallel, hierarchically interconnected cortico-BG-thalamic loops. Based on Hebbian-like and three-factor learning rules, prefrontal loops learn to flexibly control WM while a motor loop learns to decide between a set of possible responses. By teaching the 1-2-AX problem to the model, we have shown a formal task comparable to one in a shared workspace scenario.

In future work, we could extend the model to simulate reward based guidance of vision. In such a model, the agent will not push two buttons, but it will be able to look at different objects. This will result in an even closer integration between the object recognition system and the working memory model. The possibility to actively guide vision will enhance the recognition in a lot of situations, for example to recognize an object on a very cluttered office desk. In this proposed model, a loop though basal ganglia and

ITC will reinforce some cell in ITC relevant for the task at hand. These ITC cells will then project back to HVA and activate specific features (feature-based attention, [3, 6]). By the FEF, the feature based attention will result in a spatial attention encoding a saccade target in FEF movement part.

References

[1] H. Schroll, J. Vitay and F.H. Hamker, Working memory and response selection: A computational account of interactions among cortico-basal ganglio-thalamic loops, Submitted (2011).

[2] J. Vitay, F.H. Hamker, A computational model of the influence of basal ganglia on memory retrieval in rewarded visual memory tasks, Frontiers in Computational Neuroscience 4(13) (2010), 1-18.

[3] F. Beuth, J. Wiltschut and F.H. Hamker, Attentive Stereoscopic Object Recognition, in: Machine Learning reports 04/2010, AG Computational Intelligence, University of Leipzig. (2010), 41-48.

[4] J. Vitay and F.H. Hamker, Eyeshots Deliverable D3.3a - Working Memory Model, (2010).

[5] F. Beuth, J. Wiltschut and F.H. Hamker, Eyeshots Deliverable D3.2 - Object-based top-down selection using learned bi-directional connections between feature detectors to localize the object of interest in a cluttered 3D scene, (2010).

[6] F.H. Hamker, The emergence of attention by population-based inference and its role in distributed processing and cognitive control of vision, Comp Vis Image Understand 100 (2005), 64-106.

[7] A.D. Baddeley, G. Hitch, Working memory, in: G. A. Bower (Ed.), The Psychology of Learning and Motivation, Academic Press London, (1974), 48-79.

[8] G. Repovs, A. Baddeley, The multi-component model of working memory: Explorations in experimental cognitive psychology, Neuroscience 139 (2006), 5-21.

[9] W.H. Overman, Performance on traditional matching to sample, non-matching to-sample, and object discrimination tasks by 12-to-32-month-old children: a developmental progression, in: A. Diamond (Ed.), Development and Neural Bases of Higher Cognitive Functions, Academy of Sciences Press, New York, (1990), 365-393.

[10] M. Luciana, C.A. Nelson, The functional emergence of prefrontally-guided working memory systems in four- to eight-year-old children, Neuropsychologia 36(3) (1998), 273-293.

[11] C.E. Curtis, M. D'Esposito, Persistent activity in the prefrontal cortex during working memory, Trends in Cognitive Sciences 7(9) (2003), 415-423.

[12] D. Passingham, K. Sakai, The prefrontal cortex and working memory: physiology and brain imaging, Current Opinion in Neurobiology 14 (2004), 163-168.

[13] J.B. Rawney, C. Constantinidis, Neural correlates of learning and working memory in the primate posterior parietal cortex, Neurobiology of Learning and Memory 91 (2009), 129-138.

[14] J. Jonides, E.H. Schumacher, E.E. Smith, R.A. Koeppe, E. Awh, P.A. Reuter-Lorenz, C. Marshuetz, C.R. Willis, The role of parietal cortex in verbal working memory, The Journal of Neuroscience 18(13) (1998), 5026-5034.

[15] C.M. Bird, N. Burgess, The hippocampus and memory: insights from spatial processing, Nature Reviews Neuroscience 9 (2008), 182-194.

[16] G. Ben-Yehudah, S. Guediche, J.A. Fiez, Cerebellar contributions to verbal working memory: beyond cognitive theory, The Cerebellum 6 (2007), 193-201.

[17] L.L. Brown, J.S. Schneider, T.I. Lidskyz, Sensory and cognitive functions of the basal ganglia, Current Opinion in Neurobiology 7 (1997), 157-163.

[18] F.A. Middleton, P.L. Strick, Basal ganglia and cerebellar loops: motor and cognitive circuits, Brain Research Reviews 31 (2000), 236-250.

[19] S.N. Haber, The primate basal ganglia: parallel and integrative networks, Journal of Chemical Neuroanatomy 26 (2003), 317-330.

[20] P. Voorn, L. Vanderschuren, H.J. Groenewegen, T.W. Robbins, C. Pennartz, Putting a spin on the dorsal-ventral divide of the striatum, Trends in Neurosciences 27 (2004), 468-474.

[21] C.A. Seger, How do the basal ganglia contribute to categorization? Their roles in generalization, response selection, and learning via feedback, Neuroscience and Biobehavioral Reviews 32 (2008), 265-278.

[22] H.H. Yin, B.J. Knowlton, The role of the basal ganglia in habit formation, Nature Reviews Neuroscience 7 (2006), 464-476.

[23] F.G. Ashby, B.O. Turner, J.C. Horvitz, Cortical and basal ganglia contributions to habit learning and automaticity, Trends in Cognitive Sciences 14(5) (2010), 208-215.

[24] M.G. Packard, B.J. Knowlton, Learning and memory functions of the basal ganglia, Annual Review of Neuroscience 25 (2002), 563-593.

[25] W. Schultz, P. Dayan, P.R. Montague, A neural substrate of prediction and reward, Science 275 (1997), 1593–1599.

[26] J.R. Hollerman, W. Schultz, Dopamine neurons report an error in the temporal prediction of reward during learning, Nature Neuroscience 1(4) (1998), 304-309.

[27] W. Schultz, Getting formal with dopamine and reward, Neuron 36 (2002), 241-263.

[28] J.N. Reynolds, B.I. Hyland, J.R. Wickens, A cellular mechanism of reward-related learning, Nature 413 (2001), 67-70.

[29] D.J. Surmeier, J. Ding, M. Day, Z. Wang, W. Shen, D1 and D2 dopamine-receptor modulation of striatal glutamatergic signaling in striatal medium spiny neurons, Trends in Neurosciences 30 (2007), 228-235.

[30] W. Shen, M. Flajolet, P. Greengard, J. Surmeier, Dichotomous dopaminergic control of striatal synaptic plasticity, Science 321 (2008), 848-851.

[31] F.G. Ashby, J.M. Ennis, B.J. Spiering, A neurobiological theory of automaticity in perceptual categorization, Psychological Review 114(3) (2007), 632-656.

[32] M.R. DeLong, T. Wichmann, Circuits and circuit disorders of the basal ganglia, Archives of Neurology 64 (2007), 20-24.

[33] R.C. O'Reilly, M.J. Frank, Making working memory work: A computational model of learning in the prefrontal cortex and basal ganglia, Neural Computation 18 (2006), 283-328.

[34] N. Chumerin, Nikolay Chumerin's myRaytracer,
Online Resource: http://sites.google.com/site/chumerin/projects/myraytracer, (2009).

[35] I. Ohzawa, G. C. DeAngelis and R. D. Freeman, Stereoscopic depth discrimination in the visual cortex: neurons ideally suited as disparity detectors, Science 249 (1990), 1037-41.

[36] N. Qian, Computing Stereo Disparity and Motion with Known Binocular Cell Properties, Neural Computation 6 (1994), 390-404.

[37] J. C. A. Read and B. G. Cumming, Sensors for impossible stimuli may solve the stereo correspondence problem, Nat Neurosci 10 (2007), 1322-8.

[38] S.P. Sabatini, G. Gastaldi, F. Solari, J. Diaz, E. Ros K. Pauwels, M.M. Van Hulle, N. Pugeault and N. Krüger, Compact and Accurate Early Vision Processing in the Harmonic Space, International Conference on Computer Vision Theory and Applications (VISAPP), Barcelona (2007).

[39] J. Wiltschut and F.H. Hamker, Efficient coding correlates with spatial frequency tuning in a model of V1 receptive field organization, Vis Neurosci 26 (2009), 21-34.

[40] P. Földiàk, Learning invariance from transformation sequences, Neural Computation 3 (1991), 194-200.

[41] E. T. Rolls and S. M. Stringer, Invariant object recognition in the visual system with error correction and temporal difference learning. Network 12 (2001), 111-129.

[42] G. Wallis and E. T. Rolls, Invariant face and object recognition in the visual system, Prog Neurobiol 51 (1997), 167-194.

[43] K.A. Krueger, P. Dayan, Flexible shaping: How learning in small steps helps, Cognition 110 (2009), 380-394.

[44] G.E. Alexander, M.R. DeLong, P.L. Strick, Parallel organization of functionally segregated circuits linking the basal ganglia and cortex, Annual Review of Neuroscience 9 (1986), 357-381.

[45] M.D. Humphries, T.J. Prescott, The ventral basal ganglia, a selection mechanism at the crossroads of space, strategy, and reward, Progress in Neurobiology 90(4) (2010), 385-417.

[46] P. Redgrave, M. Rodriguez, Y. Smith, M.C. Rodriguez-Oroz, S. Lehericy, H. Bergman, Y. Agid, M.R. DeLong, J.A. Obeso, Goal-directed and habitual control in the basal ganglia: implications for Parkinson's disease, Nature Reviews Neuroscience 11(11) (2010), 760-772.

[47] J.C. Horvitz, Stimulus-response and response-outcome learning mechanisms in the striatum, Behavioural Brain Research 199(1) (2009), 129-140.

[48] M. Takada, H. Tokuno, A. Nambu, M. Inase, Corticostriatal projections from the somatic motor areas of the frontal cortex in the macaque monkey: segregation versus overlap of input zones from the primary motor cortex, the supplementary motor area, and the premotor cortex, Experimental Brain Research 120 (1998), 114-128.

[49] M. Inase, S.T. Sakai, J. Tanji, Overlapping corticostriatal projections from the supplementary motor area and the primary motor cortex in the macaque monkey: an anterograde double labeling study, The Journal of Comparative Neurology 373 (1996), 283-296.

[50] R. Calzavara, P. Mailly, S.N. Haber, Relationship between the corticostriatal terminals from areas 9 and 46, and those from area 8A, dorsal and rostral premotor cortex and area 24c: an anatomical substrate for cognition to action, European Journal of Neuroscience 26 (2007), 2005-2024.

[51] H. Braak, K. Del Tredici, Cortico-basal ganglia-cortical circuitry in Parkinson's disease reconsidered, Experimental Neurology 212 (2008), 226-229.

[52] F.G. Ashby, S.W. Ell, V.V. Valentin, M.B. Casale, FROST: A distributed neurocomputational model of working memory maintenance, Journal of Cognitive Neuroscience, 17(11) (2005), 1728-1743.

[53] J.N. Reynolds, J.R. Wickens, Dopamine-dependent plasticity of corticostriatal synapses, Neural Networks 15 (2002), 507-521.

[54] R. Kötter, Postsynaptic integration of glutamatergic and dopaminergic signals in the striatum, Progress in Neurobiology 44 (1994), 163-196.

[55] T. Suzuki, M. Miura, K. Nishimura, T. Aosaki, Dopamine-dependent synaptic plasticity in the striatal cholinergic interneurons, The Journal of Neuroscience 21(17) (2001), 6492-6501.

[56] C. Cepeda, C.S. Colwell, J.N. Itri, S.H. Chandler, M.S. Levine, Dopaminergic modulation of NMDA-induced whole cell currents in neostriatal neurons in slices: contribution of calcium conductances, Journal of Neurophysiology 79 (1998), 82-94.

[57] K.C. Martin, M. Barad, E.R. Kandel, Local protein synthesis and its role in synapse-specific plasticity, Current Opinion in Neurobiology 10 (2000), 587-592.

[58] S. Cervenka, L. Bäckman, Z. Cselényi, C. Halldin, L. Farde, Associations between dopamine D2-receptor binding and cognitive performance indicate functional compartmentalization of the human striatum, NeuroImage 40 (2008), 1287-1295.

[59] M.A. Piggott, E.F. Marshall, N. Thomas, S. Lloyd, J.A. Court, E. Jaros, D. Costa, R.H. Perry, E.K. Perry, Dopaminergic activities in the human striatum: rostrocaudal gradients of uptake sites and of D1 and D2 but not of D3 receptor binding of dopamine, Neuroscience 90 (1999), 433-445.

[60] A.M. Owen, N.J. Herrod, D.K. Menon, J.C. Clark, S.P. Downey, T.A. Carpenter, P.S. Minhas, F.E. Turkheimer, E.J. Williams, T.W. Robbins, B.J. Sahakian, M. Petrides, J.D. Pickard, Redefining the functional organization of working memory processes within human lateral prefrontal cortex, European Journal of Neuroscience 11 (1999), 567-574.

[61] C.M. Stinear, J.P. Coxon, W.D. Byblow, Primary motor cortex and movement prevention: Where Stop meets Go, Neuroscience and Biobehavioral Reviews 33 (2009), 662-673.

[62] J. Vitay, F.H. Hamker, Sustained activities and retrieval in a computational model of the perirhinal cortex, Journal of Cognitive Neuroscience 20(11) (2008), 1993-2005.

[63] J. Tanji, E. Hoshi, Role of the lateral prefrontal cortex in executive behavioral control, Physiological Reviews 88 (2008), 37-57.

[64] M.G. Feenstra, M.H. Botterblom, Rapid sampling of extra-cellular dopamine in the rat prefrontal cortex during food consumption, handling and exposure to novelty, Brain Research 742 (1996), 17-24.

[65] R.W. Guillery, S.M. Sherman, Thalamic relay functions and their role in corticocortical communication: Generalizations from the visual system, Neuron 33 (2002), 163-175.

[66] A. Hirata, A. Castro-Alamancos, Neocortex network activation and deactivation states controlled by the thalamus, Journal of Neurophysiology 103 (2010), 1147-1157.

[67] D.S. Melchitzky, D.A. Lewis, Dopamine transporter-immunoreactive axons in the mediodorsal thalamic nucleus of the macaque monkey, Neuroscience 103 (2001), 1033-1042.

[68] M.Á. Sánchez-González, M.Á García-Carbezas, B. Rico, C. Cavada, The primate thalamus is a key target for brain dopamine, The Journal of Neuroscience 25(26) (2005), 6076-6083.

[69] S. Miyachi, X. Lu, M. Imanishi, K. Sawada, A. Nambu, M. & Takada, Somatotopically arranged inputs from putamen and subthalamic nucleus to primary motor cortex, Neuroscience Research 56 (2006), 300-308.

[70] A. Ebrahimi, R. Pochet, M. Roger, Topographical organization of the projections from physiologically identified areas of the motor cortex to the striatum in the rat, Neuroscience Research 14 (1992), 39-60.

[71] J.M. Tepper, GABAergic Interneurons of the Striatum, in: H. Steiner, K. Tseng (Eds.), Handbook of Basal Ganglia Structure and Function, Academic Press London (2010), 151-166.

[72] M.R. Delgado, M.M. Miller, S. Inati, E.A. Phelps, An fMRI study of reward-related probability learning, NeuroImage 24 (2005), 862-873.

[73] R.E. Featherstone, R.J. McDonald, Dorsal striatum and stimulus-response learning: Lesions of the dorsolateral, but not dorsomedial, striatum impair acquisition of a stimulus-response-based instrumental discrimination task, while sparing conditioned place preference learning, Neuroscience 124 (2004), 23-31.

[74] A. Nambu, H. Tokuno, M. Takada, Functional significance of the cortico-subthalamo-pallidal 'hyperdirect' pathway, Neuroscience Research 43 (2002), 111-117.

[75] A. Parent, L.-N. Hazrati, Functional anatomy of the basal ganglia. II. The place of subthalamic nucleus and external pallidum in basal ganglia circuitry, Brain Research Reviews 20 (1995), 128-154.

[76] G. Kleiner-Fisman, J. Herzog, D.N. Fisman, F. Tamma, K.E. Lyons, R. Pahwa, A.E. Lang, G. Deuschl, Subthalamic Nucleus Deep Brain Stimulation: Summary and meta-analysis of outcomes, Movement Disorders 21(14) (2006), 290-304.

[77] M. Alegret, C. Junque, F. Valldeoriola, P. Vendrell, P. Pilleri, J. Rumià, E. Tolosa, Effects of bilateral subthalamic stimulation on cognitive function in Parkinson disease, Archives of Neurology 58 (2001), 1223-1227.

[78] K. Witt, U. Pulkowski, J. Herzog, D. Lorenz, W. Hamel, G. Deuschl, P. Krack, Deep brain stimulation of the subthalamic nucleus improves cognitive flexibility but impairs response inhibition in Parkinson disease, Archives of Neurology 61 (2004), 697-700.

[79] T. Hershey, J. Wu, P.M. Weaver, D.C. Perantie, M. Karimi, S.D. Tabbal, J.S. Perlmutter, Unilateral vs. bilateral STN DBS effects on working memory and motor function in Parkinson disease, Experimental Neurology 210 (2008), 402-408.

[80] J.L. Alberts, C. Voelcker-Rehage, K, Hallahan, M. Vitek, R. Bamzai, J.L. Vitek, Bilateral subthalamic stimulation impairs cognitive - motor performance in Parkinson's disease patients, Brain 131 (2008), 3348-3360.

[81] H. Kita, Y. Tachibana, A. Nambu, S. Chiken, Balance of monosynaptic excitatory and disynaptic inhibitory responses of the Globus Pallidus induced after stimulation of the Subthalamic Nucleus in the monkey, The Journal of Neuroscience 25(38) (2005), 8611-8619.

[82] M.R. DeLong, Primate models of movement disorders of basal ganglia origin, Trends in Neurosciences 13(7) (1990), 281-285.

[83] G.E. Alexander, M.D. Crutcher, Functional architecture of basal ganglia circuits: Neural substrates of parallel processing, Trends in Neurosciences 13(7) (1990), 266-271.

[84] J.A: Obeso, M.C. Rodriguez-Oroz, F.J. Blesa, J. Gurid, The globus pallidus pars externa and Parkinson's disease. Ready for prime time?, Experimental Neurology 202 (2006), 1-7.

[85] G. Chevalier, J.M. Deniau, Disinhibition as a basic process in the expression of striatal functions, Trends in Neurosciences 13 (1990), 277-280.

[86] H. Lange, G. Thorner, A. Hopf, Morphometric-statistical structure analysis of human striatum, pallidum, and nucleus subthalamicus: III. Nucleus subthalamicus, Journal f ür Hirnforschung 17 (1976), 31-41.

[87] J.W. Brown, D. Bullock, S. Grossberg, How the basal ganglia use parallel excitatory and inhibitory learning pathways to selectively respond to unexpected rewarding cues, The Journal of Neuroscience 19(23) (1999), 10502-10511.

[88] D. Joel, I. Weiner, The connections of the dopaminergic system with the striatum in rats and primates: An analysis with respect to the functional and compartmental organization of the striatum, Neuroscience 96 (2000), 451-474.

[89] W. Matsuda, T. Furuta, K.C. Nakamura, H. Hioki, F. Fujiyama, R. Arai, T. Kaneko, Single nigrostriatal dopaminergic neurons form widely spread and highly dense axonal arborizations in the neostriatum, The Journal of Neuroscience 29(2) (2009), 444-453.

[90] N.B. Reese, E. Garcia-Rill, R.D. Skinner, The pedunculopontine nucleus: auditory input, arousal and pathophysiology, Progress in Neurobiology 42 (1995), 195-133.

[91] P. Winn, How best to consider the structure and function of the pedunculopontine tegmental nucleus: Evidence from animal studies, Journal of the Neurological Sciences 248 (2006), 234-250.

[92] G. Di Giovanni, W.-X. Shi, Effects of scopolamine on dopamine neurons in the substantia nigra: role of the pedunculopontine tegmental nucleus, Synapse 63 (2009), 673-680.

[93] J. Mena-Segovia, J.P. Bolam, P.J. Magill, Pedunculopontine nucleus and basal ganglia: distant relatives or part of the same family?, Trends in Neurosciences 27(10) (2004), 585-588.

[94] C.B. Holroyd, M.G.H. Coles, The neural basis of human error processing: reinforcement learning, dopamine, and the error-related negativity, Psychological Review 109 (2002), 679-709.